

# Fundamental suppression of backscattering in silicon microrings

ANG LI<sup>1,2,\*</sup> AND WIM BOGAERTS<sup>1,2</sup>

<sup>1</sup>Photonics Research Group, Ghent University-IMEC, Department of Information Technology, 9052 Gent, Belgium

<sup>2</sup>Center for Nano and Biophotonics (NB-Photonics), Ghent University, 9052 Gent, Belgium

\*ang.li@ugent.be

**Abstract:** In this paper we theoretically prove and experimentally demonstrate a novel approach to eliminate the effects of backscattering in silicon ring resonators. Not only the resonance-splitting can be completely suppressed, but also the unwanted light reflected to the *in* port and directed to the *add* port can be dramatically reduced. Ring resonators have become one of the most intensively used integrated optical components for various applications. However, in high-index-contrast platforms like silicon photonics, sidewall roughness induced backscattering imposes limits on the performance of ring resonators. It frequently induces resonance-splitting in *through* and *drop* ports. At the same time, there will be unwanted light directed to the *add* port and reflected to the *in* port. We show that, by putting an intentional tunable reflector inside the ring to compete with the stochastic backscattering, the ring can work under a normal condition. All resonances can be tuned to be non-split with an improved extinction ratio and there will be significantly less light coming out from the *in* and the *add* ports.

© 2017 Optical Society of America

**OCIS codes:** (290.1350) Backscattering; (130.3120) Integrated optics devices; (140.4780) Optical resonators; (230.7020) Traveling-wave devices; (130.7408) Wavelength filtering devices.

## References and links

1. V. R. Almeida, C. A. Barrios, R. R. Panepucci, and M. Lipson, "All-optical control of light on a silicon chip," *Nature* **431**, 1081–1084 (2004).
2. K. De Vos, I. Bartolozzi, E. Schacht, P. Bienstman, and R. Baets, "Silicon-on-Insulator microring resonator for sensitive and label-free biosensing," *Opt. Express* **15**, 7610–7615 (2007).
3. S. Gulde, A. Jebali, and N. Moll, "Optimization of ultrafast all-optical resonator switching," *Opt. Express* **13**, 9502–9515 (2005).
4. Q. Xu, B. Schmidt, S. Pradhan, and M. Lipson, "Micrometre-scale silicon electro-optic modulator," *Nature* **435**, 325–327 (2005).
5. W. Bogaerts, P. De Heyn, T. Van Vaerenbergh, K. De Vos, S. Kumar Selvaraja, T. Claes, P. Dumon, P. Bienstman, D. Van Thourhout, and R. Baets, "Silicon microring resonators," *Laser Photon. Rev.* **6**, 47–73 (2012).
6. R. G. Beausoleil, "Large-scale integrated photonics for high-performance interconnects," *J. Emerg. Technol. Comput. Syst.* **7**, 6:1–6:54 (2011).
7. C. Sun, M. T. Wade, Y. Lee, J. S. Orcutt, L. Alloatti, M. S. Georgas, A. S. Waterman, J. M. Shainline, R. R. Avizienis, S. Lin, B. R. Moss, R. Kumar, F. Pavanello, A. H. Atabaki, H. M. Cook, A. J. Ou, J. C. Leu, Y. Chen, K. Asanovic, R. J. Ram, M. A. Popović and V. M. Stojanović, "Single-chip microprocessor that communicates directly using light," *Nature* **528**, 534–538 (2015).
8. F. Grillot, L. Vivien, S. Laval, D. Pascal, and E. Cassan, "Size influence on the propagation loss induced by sidewall roughness in ultrasmall soi waveguides," *IEEE Photon. Technol. Lett.* **16**, 1661–1663 (2004).
9. F. Morichetti, A. Canciamilla, C. Ferrari, M. Torregiani, A. Melloni, and M. Martinelli, "Roughness induced backscattering in optical silicon waveguides," *Phys. Rev. Lett.* **104**, 1–4 (2010).
10. A. Li, T. Vaerenbergh, P. Heyn, P. Bienstman, and W. Bogaerts, "Backscattering in silicon microring resonators: a quantitative analysis," *Laser Photon. Rev.* **10**, 420–431 (2016).
11. F. Morichetti, A. Canciamilla, M. Martinelli, A. Samarelli, R. M. De La Rue, M. Sorel, and A. Melloni, "Coherent backscattering in optical microring resonators," *Appl. Phys. Lett.* **96**, 13–15 (2010).
12. A. Li, Q. Huang, and W. Bogaerts, "Design of a single all-silicon ring resonator with a 150 nm free spectral range and a 100 nm tuning range around 1550 nm," *Photon. Res.* **4**, 84–92 (2016).
13. S. Werquin, S. Verstuyft, and P. Bienstman, "Integrated interferometric approach to solve microring resonance splitting in biosensor applications," *Opt. Express* **21**, 16955–16963 (2013).
14. Q. Huang, K. Ma, and S. He, "Experimental demonstration of single mode-splitting in microring with bragg gratings," *IEEE Photon. Technol. Lett.* **27**, 1402–1405 (2015).

15. A. Arbabi, Y. M. Kang, C.-Y. Lu, E. Chow, and L. L. Goddard, "Realization of a narrowband single wavelength microring mirror," *Appl. Phys. Lett.* **99**, 091105 (2011).
16. M. Fiers, T. V. Vaerenbergh, K. Caluwaerts, D. V. Ginste, B. Schrauwen, J. Dambre, and P. Bienstman, "Time-domain and frequency-domain modeling of nonlinear optical components at the circuit-level using a node-based approach," *J. Opt. Soc. Am. B* **29**, 896–900 (2012).
17. P. Dumon, W. Bogaerts, R. Baets, J.-M. Fedeli, and L. Fulbert, "Towards foundry approach for silicon photonics: silicon photonics platform epiFab," *Electron. Lett.* **45**, 581–582 (2009).

## 1. Introduction

In the past decades, numerous applications relying on ring resonators have been demonstrated, varying from WDM filters, laser cavities, optical sensors, optical logic, and modulators [1–5]. The ring resonator's popularity is mainly attributed to its high Q factor, narrow bandwidth, compact size and large extinction ratio. The use of silicon photonics further reduces the footprint of a ring resonator, enables large scale fabrication and high density integration, which are key advantages for applications requiring large numbers of resonators (e.g. optical interconnects [6, 7]). However, one problem associated with a high index contrast platform such as silicon photonics is sidewall roughness, which not only introduces additional propagation loss but also stochastic backscattering [8, 9]. These two effects, especially the second one, have been extensively studied and proven to be a key performance limiter in silicon ring resonators [10, 11]. The details regarding the effects of backscattering in silicon ring resonators are given in [10]. Backscattering, together with parasitic reflections caused by the directional couplers, will couple the clockwise propagating mode (CW) and counter-clockwise propagating mode (CCW) in the ring waveguide. For a ring resonator with a high Q factor, which is often the case, this will lead to resonance splitting in both *through* and *drop* ports, as shown in Fig. 1. Meanwhile, this will cause unwanted light reflected to the *in* port and leaked to the *add* port, also evident in Fig. 1. The percentage of split resonances can be as high as 80% [10]. Also, the resonance splitting can be asymmetric; the reason for this is proven to be the backcoupling of the directional couplers [10]. Moreover, we have also proven that the reflection will dramatically decrease the extinction ratio of the ring resonator if its resonance is close to the critical coupling condition [12]. Due to the degradation of the resonance, many ring resonator based applications will suffer from this effect. For instance, the correct resonance shift of ring based optical (bio)sensors cannot be reliably extracted by measuring a split resonance; a single mode laser with an external ring resonator cavity cannot work well if the resonance shape shows a splitting; the backreflection from a ring resonator to a laser will induce instability to the laser or even kill it.

While the phenomenon of resonance splitting has been extensively reported, there have been very few reports on how to eliminate the splitting due to the backscattering. Werquin et al. [13] have proposed an approach based on the interference of light from the pass port and the reflection of the ring resonator. By tuning the relative optical length of these two paths, one peak of the split-resonance will be suppressed. However, it works only for an individual resonance. Besides, the corrected resonance, even if it's non-split, has a lower quality compared to the original resonance in terms of extinction ratio. What's more, the backreflection cannot be fixed in this way. Another drawback is that this solution only works for *through* port, thus for the all-pass ring resonator configuration.

Instead of compensating the splitting with an external interferometer, our approach compensates the backscattering inside the ring resonator by introducing a tunable reflector. This compensates both the distributed CW-CCW coupling by the sidewall roughness and lumped coupling at the directional couplers. Adding a reflector inside a ring resonator has been demonstrated using a Bragg mirror [14, 15], but these mirrors are hardly tunable, and cannot be used for the compensation of backscattering.

In this paper, we present a ring with an integrated tunable reflector. We show that we can completely eliminate the resonance splitting in all output ports of both all-pass and add-drop

configurations. The unwanted transmission to the *add* port and reflection to the *in* port can also be dramatically suppressed.

In the following sections, we will first propose our idea to compensate backscattering inside the ring resonator and show some simulation results. After that, experimental results will be given. Finally we discuss the limitations of this device and conclude this work.

## 2. Theory and simulation

A very comprehensive and in-depth analysis of backscattering in silicon ring resonators is already presented in [10]. A good model that can explain and predict the different types and shapes of resonance-splitting is also constructed. With the help of that model, we get to know that the total backscattering can be simply represented by a reflector with a given reflectivity and phase. Naturally if we can take control of the total reflectivity inside the ring, we can then fully control the resonance shape. In order to do so, we need an integrated reflector to be put inside the ring that can be dominant over the backscattering. The reflector should be widely tunable as the backscattering itself is quite stochastic, making it impossible to accurately know its reflectivity and phase.

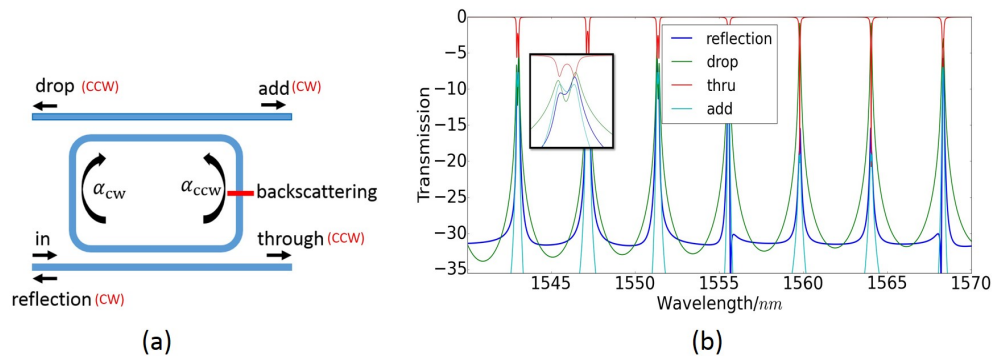


Fig. 1. (a) shows a brief schematic for a ring resonator with backscattering, which is modelled by a lumped reflector. (b) gives the simulated spectra of such a ring resonator to demonstrate the effects of backscattering in the circuit. Note the clear resonance splitting in *through* and *drop* port, and the high transmission in *add* port and *in* port.

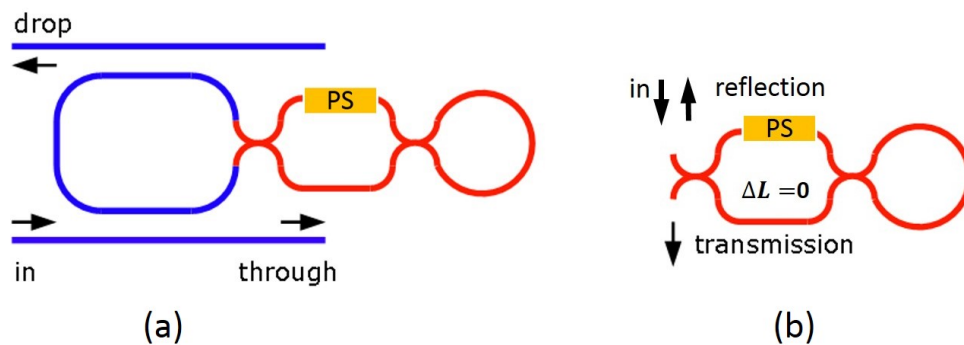


Fig. 2. Schematics of the ring with a reflector and the reflector itself, respectively.

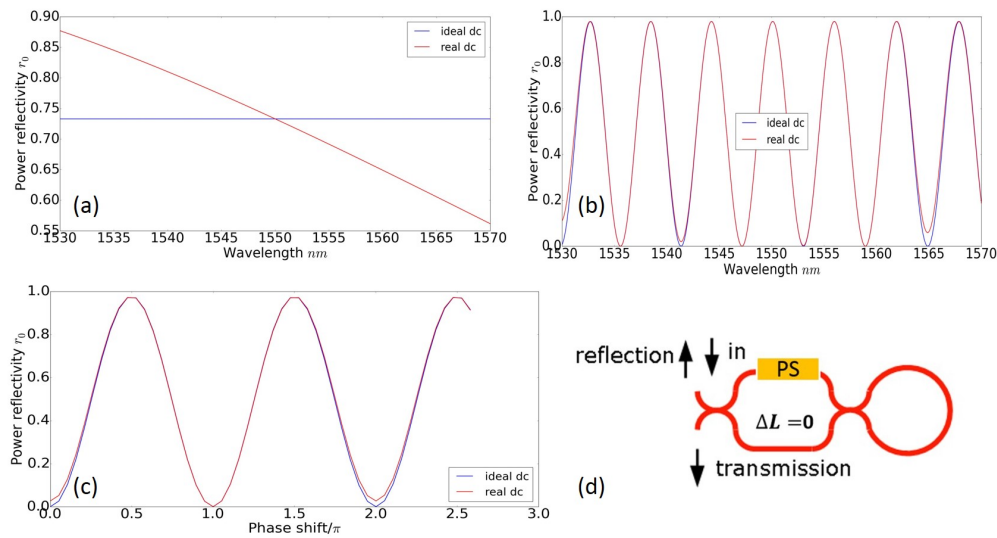


Fig. 3. Simulated reflection spectrum of the tunable reflector. (a)  $\Delta L = 0$  produces a flat spectrum. (b)  $\Delta L = 50$  shows a strong, periodic wavelength dependence oscillating between 0 and 100%. (c) Adding  $0.5\pi$  phase shift in one arm can generate a change in reflectivity from 0 to 100%. Blue and red corresponds with an ideal directional coupler case and a realistic directional coupler case, respectively. The reflection does not reach 100% because of the small propagation loss of the waveguides which is taken into account. (d) shows the reflector with a phase shifter used to simulate the tunability.

### 3. Experiment results

The schematics of our device and the reflector itself are shown in Fig. 2. It is a Mach-Zehnder Interferometer (MZI) with a loop end. By designing the length difference  $\Delta L$  of the MZI, we can obtain quite diverse reflection spectra. With  $\Delta L = 0$ , the spectrum is relatively flat, otherwise it shows a periodic wavelength dependence, as indicated in Fig. 3. These transmission/reflection curves are simulated by the optical circuit simulator *Caphe* [16]. We simulated the loop mirror where the directional couplers (DCs) are supposed to have an ideal 50/50 splitting ratio with no wavelength dependence, and a circuit where DCs have a linear wavelength dependency (in reality, the wavelength dependency of a DC is more complicated than linear. But a linear dependency here is accurate enough to show the influence of DC on the reflector's performance. Any higher-order dependency does not affect our analysis in any substantial way). The dispersive behavior of directional couplers will slightly influence both reflection spectrum and its tunability as evident in Fig. 3. Still, the tunable reflector will always have a point of zero reflectivity.

In terms of its tunability, only  $0.5\pi$  phase shift in any of the two MZI arms will result in a change in reflectivity from 0 to almost 100% (the reflector has some loss due to the waveguide propagation). This can be easily achieved by thermo-optic tuning with relatively low power consumption. The simulation results from *Caphe* are shown in Fig. 3(d).

In order to test our hypothesis, we built a circuit model for a ring resonator with backscattering in *Caphe*. According to our model presented in [10], backscattering can be treated as a lumped reflector with a constant reflectivity but a random phase. The results of this circuit without and with our reflector are shown in Fig. 4. Obviously, without the intentional reflector, the spectrum shows resonance-splitting due to the existence of backscattering. The asymmetry in some split resonances can be attributed to additional parasitic effects, namely reflections and backcoupling at the directional couplers [10]. By introducing our reflector and adjusting the phase in one arm,

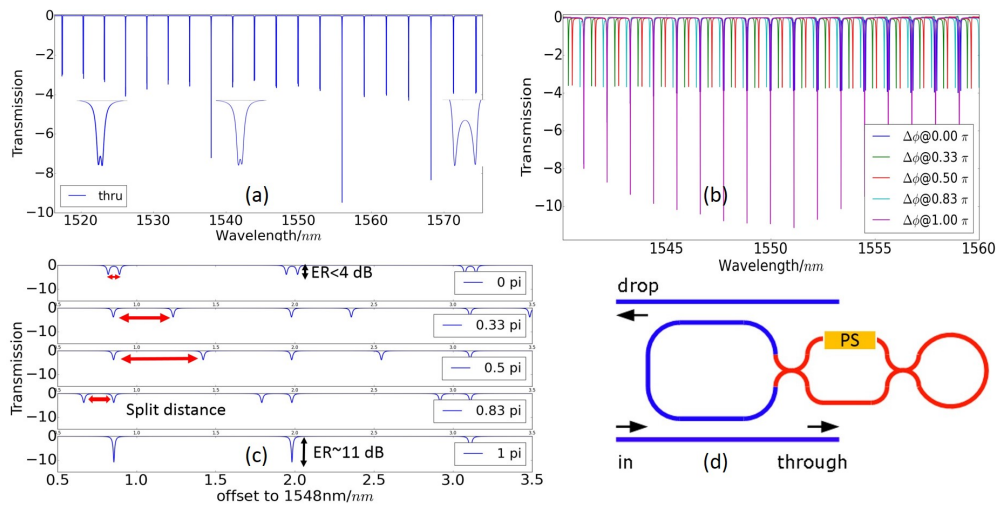


Fig. 4. Simulated through port spectrum of a ring circuit with only backscattering and other parasitics in the circuit, including reflections and backcoupling at the directional couplers (a), and with both backscattering and tunable reflector (b) and (c). It shows clearly how the resonance shape evolves with phase shift. (d) gives the brief schematic of the device with a phase shifter.

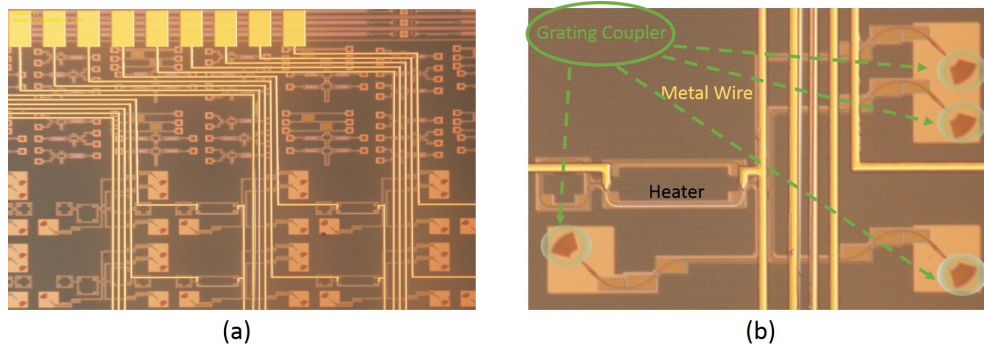


Fig. 5. (a) gives the overall view of the devices fabricated after heater processing. (b) presents a zoomed view of one specific device.

the total reflectivity inside the ring can be controlled: the resonance shape evolves from visibly split to non-split. And note that, during the modulation period, one of the resonance wavelengths hardly changes. The principle behind this is simple. The resonance splitting will create two peaks on both sides of the original resonance. One is blue shifted ( $R_b$ ) and the other one is red shifted ( $R_r$ ), with a separation that depends linearly on the coupling strength between the CW and CCW propagating modes, and this is given by the reflectivity of the cavity reflector [10]. The phase shift of the tuner in the MZI reflector will also add an increment to the total optical length of the ring, thus leading to a redshift of the entire spectrum (both  $R_b$  and  $R_r$ ). At the same time this phase shift will increase the reflectivity, and thus  $R_b$  will experience an additional blueshift due to the increase of the separation, effectively cancelling the redshift and keeping  $R_b$  in place. For the redshifted resonance  $R_r$ , the two effects add up.

When the phase shift in the MZI induces the maximum, near-100% reflectivity (or 0% transmission), the peak separation is maximum, at half the FSR of the original ring resonator: the

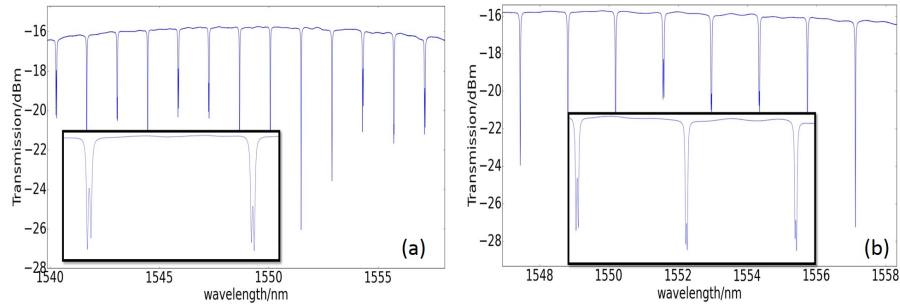


Fig. 6. Two measured spectra of simple ring resonators (without reflectors) on the same chip, located close to the ring resonator with tunable reflector. Both rings, which have different coupling conditions, show clear resonance-splitting in most resonance peaks.

shifted resonance  $R_r$  is now exactly in between its corresponding  $R_b$  and the  $R_b$  of the adjacent resonance. This can be easily understood as now the ring cavity is cut in one place, turning it into a Fabry-Perot cavity with twice the roundtrip length. Increasing the phase shift further will start to decrease the reflectivity, but with a flip in phase ( an abrupt  $\pi$  change in phase ). This will continue to shift the  $R_r$  peak, now reducing the separation with the next resonance's  $R_b$ , eventually merging with the resonances. At that point, the phase shifters have added  $2\pi$  phase shift to the circumference of the ring, effectively increasing the order of each resonance with 1.

The phase shifter in the MZI only controls the relative positions of the split peaks. To control the absolute position of the resonances, an additional thermal tuner can be added in the main loop of the ring, or a global temperature control can be used.

The fabrication is executed on IMEC's passive silicon photonics platform through the Europractice MPW service [17]. The waveguide cross-section is designed to be  $450\text{ nm} \times 220\text{ nm}$ . The sample is covered by a planarized oxide cladding on top of which we process metal heaters for the phase shifters, as shown in Fig. 5. The heaters consist of a titanium resistive element connected with gold contact electrodes. The Ti heater has a  $2\ \mu\text{m}$  width and  $100\text{ nm}$  thickness. For the device, we choose the two arms of the MZI reflector to be identical, with a length of  $200\ \mu\text{m}$ , to make sure sufficient phase shift can be achieved. The measurement results show that  $15\text{ mW}$  can give a  $\pi$  phase shift of our heater. This is overdimensioned to demonstrate the concept: experimental results show that the length of the MZI arms can be shortened to  $100\ \mu\text{m}$ , even without the use of more efficient heaters.

As a reference to our actively compensated ring resonator we use two ring resonators without reflectors inside, located close to our device on the same chip to prove the existence and influence of actual backscattering. They are configured at different coupling conditions, and therefore their resonances have different line widths. The measured spectra in Fig. 6 clearly show how frequent the backscattering-induced resonance splitting can be and the suppression of extinction ratio of split resonances. Note that these test rings have a much shorter total length compared to our device, thus our device is expected to suffer from much stronger backscattering as the backscattering strength grows linearly with ring roundtrip length [10].

The active measurement of our device is shown in Fig. 7. As evident, by injecting current, under some condition all of the resonance shapes become non-split and the extinction ratio increases dramatically compared to the original split resonance. This is because the extinction ratio gets suppressed by reflection inside the ring [12]. We also characterized how the unwanted transmission at *in* and *add* ports will be influenced. Both spectra show a clear suppression in power and a change in shape. In detail, for the *add* port spectrum, instead of split resonance, after injecting proper current, the shape becomes non-split. This residual transmission in the

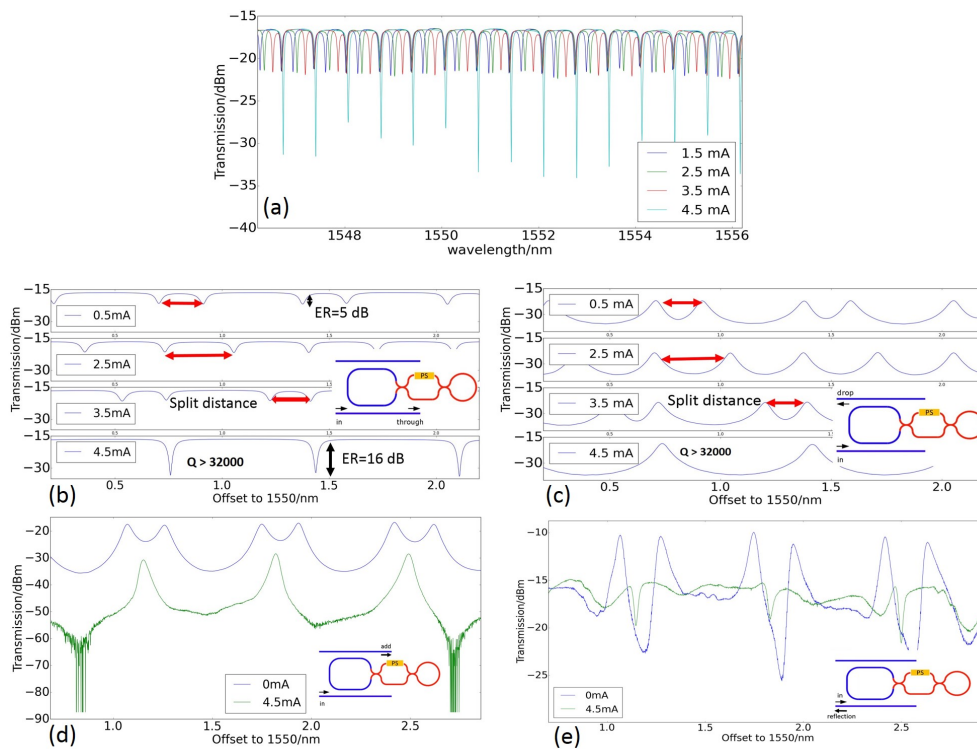


Fig. 7. Experimental measurements of compensated backscattering. (a) demonstrates the control of all the resonances. (b) gives a zoomed-in view about how the resonance shapes evolve from clearly split to non-split. (c) shows the same compensation for the output at the drop port, while (d) and (e) show how our device can suppress the unwanted output from *add* and *in* port.

*add* port is not a remaining parasitic backscattering of the ring resonator, but is caused by the parasitic reflection at the output grating coupler, which excites the clockwise ring mode from the *through* port. This actually can be considered as another confirmation of the elimination of backscattering in the ring since the resonance shape has become a clear Lorentzian-line. Similarly, in the reflection spectrum, there is originally a clearly split resonance pattern, while after current injection, the resonances disappear, with just parasitic random reflections remaining.

An additional advantage of our device, as a consequence of using the MZI loop mirror, is the fixed wavelength position of one resonance wavelength, which is clearly demonstrated by both simulation (Fig. 4) and measurement (Fig. 7). By applying a second phase shift on the other side of the ring resonator (or a global index change), one can still tune the absolute wavelength of the resonance.

We also show the measurement results at the drop port in Fig. 7. The resonance splitting exhibits the same trend in both ports of an add-drop filter, which again confirms the fact that, our solution indeed fundamentally compensates the backscattering inside the ring resonator.

#### 4. Conclusion

In this paper, we propose and experimentally demonstrate a novel approach to eliminate backscattering and resonance splitting in ring resonators, by introducing a tunable reflector. It has three significant advantages compared to former proposed method. First of all, by incorporating

a tunable reflector inside the ring, we can make all the resonances non-split. Secondly, the extinction ratio of the resonance will be recovered from resonance splitting. Finally, the unwanted light at *in* and *add* port can also be significantly suppressed.

The biggest limitation of our device is the long ring length, or in other words, the small *free spectral range* (FSR). But the device shown in this paper is not yet optimized in its total length. For instance, the MZI reflector's arm length can be safely reduced to 100-120  $\mu\text{m}$  without sacrificing performance. This will bring a 160  $\mu\text{m}$  reduction in the total ring length. Still, the lower boundary of the roundtrip length is around 350  $\mu\text{m}$ , which translates to a maximum FSR of 1.7 nm. This will limit its application as WDM filter. But it can still be valuable for applications like microwave filters, integrated optical sensors or multi-mode laser cavities.